Published as: *Cell*. 2009 May 15; 137(4): 761–772.

Essential role for TRPC5 in amygdala function and fear-related behavior

Antonio Riccio[1,2], **Yan Li**[3], **Jisook Moon**[3], **Kwang-Soo Kim**[3], **Kiersten S. Smith**[3], **Uwe Rudolph**[3], **Svetlana Gapon**[1], **Gui Lan Yao**[2], **Evgeny Tsvetkov**[3], **Scott J. Rodig**[4], **Ashlee Van't Veer**[3], **Edward G. Meloni**[3], **William A. Carlezon Jr**[3], **Vadim Y. Bolshakov**[3], and **David E. Clapham**[1,2]

[1] Department of Cardiology, Howard Hughes Medical Institute, Manton Center for Orphan Disease, Children's Hospital Boston, Boston, Massachusetts 02115

[2] Department of Neurobiology, Harvard Medical School, Boston, Massachusetts 02115

[3] Department of Psychiatry, McLean Hospital, Harvard Medical School, Belmont, Massachusetts 02478

[4] Department of Pathology, Brigham & Women's Hospital, Boston, Massachusetts 02115

Summary

The transient receptor potential channel 5 (TRPC5) is predominantly expressed in the brain where it can form heterotetrameric complexes with TRPC1 and TRPC4 channel subunits. These excitatory, non-selective cationic channels are regulated by G protein, phospholipase C-coupled receptors. Here, we show that *TRPC5*$^{-/-}$ mice exhibit diminished innate fear levels in response to innately aversive stimuli. Moreover, mutant mice exhibited significant reductions in responses mediated by synaptic activation of Group I metabotropic glutamate and cholecystokinin 2 receptors in neurons of the amygdala. Synaptic strength at afferent inputs to the amygdala was diminished in P10–P13 null mice. In contrast, baseline synaptic transmission, membrane excitability, and spike timing-dependent long-term potentiation at cortical and thalamic inputs to the amygdala were largely normal in older null mice. These experiments provide genetic evidence that TRPC5, activated via G protein-coupled neuronal receptors, has an essential function in innate fear.

INTRODUCTION

Fear encompasses both innate and learned emotional responses that are part of basic survival mechanisms. Acquired (learned) fear triggers characteristic behaviors of escape and avoidance in response to a specific, previously experienced stimulus, such as pain or the threat of pain. In contrast, innate fear is genetically encoded and does not require response learning (*e.g.*, fearful response to smell of predators). Both learned and innate fear responses are controlled by the amygdala complex comprised of several subcortical nuclei in the temporal lobe of the

Correspondence should be addressed to D.E.C. (E-mail: dclapham@enders.tch.harvard.edu) or V.Y.B. (E-mail: vadimb@mclean.harvard.edu).

SUPPLEMENTAL DATA

Supplemental Data include Supplemental Results, Supplemental Experimental Procedures, Supplemental References, and 10 figures and can be found with this article online at http://www.cell.com/cgi/content/full/

brain (Pitkanen et al., 1997; Fanselow and LeDoux, 1999; LeDoux, 2000; Davis and Whalen, 2001; Fanselow and Poulos, 2005).

Our understanding of learned fear is largely based on studies of Pavlovian fear conditioning, in which an initially neutral conditioned stimulus (CS) of any sensory modality (*e.g.*, sound) is paired with an innately aversive unconditioned stimulus (US; *e.g.* an electric foot shock; LeDoux, 2000). Plastic changes in the CS pathways contribute to learning of the CS-US association (Maren and Quirk, 2004). The lateral nucleus of the amygdala (LA) is the input for sensory stimuli from the visual, auditory, somatosensory, olfactory, and taste systems, providing the CS component during fear conditioning. Inputs from the auditory thalamus and association areas of the auditory cortex (AuD, Au1, and AuV), recruited during auditory fear conditioning, enter the LA and terminate largely in its dorsal subnucleus (LeDoux, 2000). The CS stimuli converge in the LA with the painful US arising from somatosensory cortical and thalamic areas. This convergence potentiates synaptic responses in auditory inputs to the LA, retaining memory of the CS-US pairing via mechanisms of long-term potentiation (LTP; Rogan et al., 1997; McKernan and Shinnick-Gallagher, 1997; Tsvetkov et al., 2002). The central nucleus of the amygdala (CeA) is the output region of fear conditioning circuitry, which communicates with brainstem areas controlling specific fear-related behaviors and/or physiological responses (e.g., freezing in mice) (Maren and Quirk, 2004). The neural substrates of innate fear appear to be more diffuse and are not completely known. It is clear, however, that despite a certain degree of the overlap, structural specificity exists for both innate and learned fear responses (Shumyatsky et al., 2005). The processes within the amygdala also contribute to emotional arousal during a learning event, enhancing its retention (McGaugh, 2000). Anxiety disorders may reflect dysregulation of these fear systems (Milad et al., 2006).

Most sensory inputs to principal neuronal dendrites and inhibitory GABAergic interneurons in the LA are mediated by excitatory NMDA and AMPA receptors (LeDoux, 2000; Tsvetkov et al., 2004; Shin et al., 2006). Axons from these LA neurons project to other nuclei of the amygdala (LeDoux, 2000), as well as to local circuit interneurons. Neurotransmitters and neuromodulators, such as norepinephrine, dopamine, serotonin, acetylcholine, gastrin-releasing peptide, vesicular zinc, and cholecystokinin may modulate the relative state of amygdalar activity (LeDoux, 2000; Shumyatsky et al., 2002; Bissiere et al., 2003; Kodirov et al., 2006; Meis et al., 2007).

The Transient Receptor Potentials (TRP) channels, TRPC4 and TRPC5, are homologous proteins distributed in several areas of the brain, particularly the hippocampus and amygdala. In constrast to common perception, TRP channels are not exclusive to sensory nerve endings, but are also present in epithelia as well as axons, cell bodies, and dendrites of neurons. TRPC proteins control growth cone movement in both mammalian and amphibian model systems (Bezzerides et al., 2004; Greka et al., 2003; Shim et al., 2005; Wang and Poo, 2005), but their function in synapses is not well understood. Most importantly, tetrameric TRPC and TRPV subunits form excitatory, nonselective, weakly voltage-gated ion channels that are greatly potentiated by phospholipase C linked receptors (Clapham, 2003; Clapham, 2007; Ramsey et al., 2006; Strübing et al., 2001).

In order to understand TRPC5's function in brain, we generated mice in which the *TRPC5* gene had been ablated. *TRPC5*$^{-/-}$ mice demonstrated behaviors consistent with lesser innate fear than their *wt* counterparts. These behavioral effects appear to result from the loss of CCK_2- or metabotropic glutamate-receptor activation, or potentiation of excitatory Ca^{2+}-permeant TRPC5 channels.

RESULTS

TRPC5 Expression in the Mouse Brain

Consistent with previous immunocytochemical localization of TRPC5 protein (Strübing et al., 2001), TRPC5-mRNA is abundant in the amygdala (lateral, basolateral, and central nuclei) and hippocampus. High levels of TRPC5-mRNA were detected in the CA1, CA2, and CA3 regions of the hippocampus and dentate gyrus (Figure 1A), areas that regulate fear-related behaviors through projections to the amygdala (Seidenbecher et al., 2003). Regions of the auditory cortex (AuD, Au1, and AuV) that process conditioned stimulus information bound for the LA during auditory fear conditioning (Maren and Quirk, 2004), the somatosensory cortex (S1 and S2 areas) and the parietal insular cortex, regions that transmit somatosensory unconditioned stimulus (US) information to the LA, also contain TRPC5 mRNA (Figure 1A). Finally, TRPC5 is present in the perirhinal cortex (PRh), an area involved in processing CS and somatosensory US information (Lanuza et al., 2004; LeDoux, 2000; Shi and Davis, 1999; Shumyatsky et al., 2005). Interestingly, TRPC5 mRNA was not observed in the auditory thalamus, another auditory CS area (Figure 1B).

TRPC5 was present in pyramidal neurons in both the LA and the auditory cortex, where it co-localized with the neuron-specific marker CaMKIIα (Figure 1C and Figure S1). Combined *in situ* hybridization of TRPC5-mRNA and immunohistochemical labeling of CaMKIIα shows that pyramidal neurons in the auditory cortex express TRPC5 (Figure 1D). TRPC5 was not expressed in glial cells or interneurons of the LA or auditory cortex (Figure S2A–F). These results indicate that the TRPC5 expression was limited to principal cells.

Generation of *TRPC5*$^{-/-}$ Mice

The *TRPC5* gene was ablated in mice through homologous recombination (Liu et al., 2003) using a targeting construct to delete the exon 5 genomic region encoding amino acids 412–459 within the putative 4th transmembrane domain (Figure S3A). In addition to removing coding information, this manipulation introduced both a frame shift and stop codon after the deleted segment. Successful targeting was verified by Southern blotting (data not shown); the deletion of the exon 5 region was catalyzed by Cre-recombinase and was confirmed by PCR. RT–PCR analysis of transcripts from whole brain of *wt* and mutant mice confirmed the absence of exon 5 (Figure S3 B,C). TRPC5 protein in brain microsomes of *TRPC5*$^{-/-}$ homozygous mice was not detected by Western blot in immunoprecipitation experiments. Specific TRPC5 immunoreactivity was observed in the hippocampus and the dentate gyrus of control mice, but not in matched tissues from *TRPC5*$^{-/-}$ mice (Figure S3D,E). Matings between heterozygous animals produced siblings with normal Mendelian distributions of gender and genotype. mRNA levels of TRPC1, 3, 4, 6, and 7 were not significantly altered in the whole brain of *TRPC5*$^{-/-}$ mice compared to control animals (Figure S4A–E). This suggests that there were no significant compensatory changes in the expression of these genetically and functionally related genes.

Innate Fear Responses and Conditioned Fear in TRPC5$^{-/-}$ Mice

TRPC5$^{-/-}$ mice revealed no abnormalities in weight, spontaneous behavior, neurological reflexes, or sensorimotor responses (including righting, postural reflex, ear twitch reflex, grip strength, and whisker orientation reflex). Mutant mice displayed no impairment in overall spontaneous locomotor activity (Figure 2C), indicating that basic motor functions of *TRPC5*$^{-/-}$ mice were unaffected. Although *TRPC5*$^{-/-}$ mice tended to have lower acoustic startle amplitudes (at 95, 100 and 105dB), this effect was not significant (Figure 2A). Likewise, there was no effect of genotype on activity level, sampled immediately preceding the onset of the startle stimulus (Figure 2B).

Since TRPC5's expression pattern was consistent with its role in fear-related behaviors, we assayed conditioned freezing (learned fear) using a classical single-trial fear conditioning paradigm with a relatively strong US (2s, 0.7mA foot shock; Shumyatsky et al., 2002, 2005). As shown in Figure 2D, we did not observe significant differences between control and mutant mice in conditioned freezing at 24h post-training. Surprisingly, knockout mice froze more commonly in response to the conditioned tone at 24h post-training, following 10 tone-shock pairings, when a much milder US was used (0.4mA, 0.5s; Figure S5A). This suggests that TRPC5 may participate in the mechanism of conditioned fear memory (LeDoux, 2000) under certain training conditions.

Does TRPC5 participate in innate fear, which, as opposed to learned fear, does not require conditioning to potential threats? To assess the effect of *TRPC5* gene deletion on innate fear, we analyzed *TRPC5*$^{-/-}$ mice using the elevated plus-maze, open field, social interaction, and novelty suppressed feeding tests. In the elevated plus-maze experiments, knockout mice had a significantly increased number of open- (Figure 2E), but not closed-arm entries, suggesting a reduced innate fear phenotype. In open field studies, *TRPC5*$^{-/-}$ mice spent significantly more time in the center of the arena than control mice (Figure 2F). In addition, *TRPC5*$^{-/-}$ mice entered into the aversive center of the field more frequently, confirming that *TRPC5* ablation interfered with innate fear-related behaviors. *TRPC5*$^{-/-}$ mice more frequently moved to the center area than control mice during the first 5min (P=0.004), whereas mice of both groups entered into the center with an identical rate at later times (P=0.4; Figure 2G). Both control and mutant mice movements were similar during 1h observation periods (Figure 2H). In the social interaction test, *TRPC5*$^{-/-}$ mice spent more time in the compartment where the novel mouse was confined and exhibited increased number of the nose-to-nose contacts with the novel mouse compared to control mice (Figure 2I,J). The finding that TRPC5$^{-/-}$ mice were less anxious in social interactions provides further evidence that the ablation of TRPC5 had an anxiolytic-like effect. The novelty suppressed feeding latency test, however, did not reveal differences between the genotypes (Figure S5B–E). This could reflect the fact that the novelty suppressed feeding latency test, unlike all other anxiety-probing behavioral paradigms, is not sensitive to the acute action of anxiolytic drugs (Leonardo and Hen, 2006). Together, these results suggest that *TRPC5*$^{-/-}$ mice exhibited less anxious behaviors (decreased innate fear) than their *wt* counterparts.

Synaptic Transmission and LTP in Cortical and Thalamic Inputs to the LA in TRPC5$^{-/-}$ Mice

Expression of TRPC5 mRNA in the amygdala of control mice is highest at early stages of postnatal development and declines with age (Figure S6A–D). In blinded experiments, we examined the effects of *TRPC5* gene ablation on synaptic transmission in cortical inputs to the LA in slices from younger (10–13 day-old) mice. This pathway transmits conditioned stimulus (CS) information to the amygdala during auditory fear conditioning and is essential for learned fear (Maren and Quirk, 2004). To explore the role of TRPC5 in synaptic function in cortical input to the LA, we stimulated fibers in the external capsule (LeDoux, 2000; Shin et al., 2006), and recorded excitatory postsynaptic currents (EPSCs) in LA neurons in slices from *TRPC5*$^{-/-}$ and littermate control mice (Figure S7). We found that synaptic strength was significantly diminished in slices from *TRPC5*$^{-/-}$ mice, as evidenced by a rightward shift in input-output curves relative to control slices (Figure S7A, B). This decrease in synaptic strength was associated with an increase in the magnitude of paired-pulse facilitation (PPF) recorded at 50ms interstimulus intervals (Figure S7C, D; P=0.002). Since PPF varies inversely with the basal probability of release (Pr) (Zucker and Regehr, 2002), the decrease in synaptic strength was in part due to a lower Pr. Possible changes in presynaptic excitability in *TRPC5*$^{-/-}$ mice could also contribute to the observed decreases in synaptic efficacy. There was no difference, however, between experimental groups in the frequency of miniature EPSCs (mEPSCs) (Figure S7E–G). Thus, the presence of TRPC5 does not appear to affect Ca^{2+}-independent

glutamate release. Mean mEPSC amplitude in slices from control and *TRPC5*$^{-/-}$ mice was not significantly different; Figure S7F,G), suggesting that the sensitivity of postsynaptic AMPA receptors was not affected by *TRPC5* gene ablation.

We next examined LA membrane excitability and synaptic function in slices from 4–5 week-old TRPC5$^{-/-}$ mice, corresponding to a time when TRPC5 expression had decreased by ~2 fold compared to younger animals (Figure S6A). The number of spikes generated by depolarizing current injections of increasing intensity under current-clamp conditions was indistinguishable between control and TRPC5$^{-/-}$ mice (Figure 3B,C). Synaptic strength, as assessed by input-output curves for AMPA receptor-mediated EPSCs, was also unchanged in mutant mice at either cortico-amygdala synapses (Figure 3A,D) or thalamo-amygdala synapses (Figure 3A,G). We have also tested the effect of mutation on short-term synaptic plasticity, comparing the magnitude of post-tetanic potentiation (PTP) between control and *TRPC5*$^{-/-}$ mice. To prevent LTP, PTP was induced by a 1s train of 100Hz stimulation in the presence of the NMDA receptor antagonist D-APV (50μM). As shown in Figure S8, the magnitude of PTP at thalamo-amygdala synapses was not different between control and mutant mice.

To explore further the functional role of TRPC5 in basal synaptic transmission in afferent inputs to the LA, we obtained the estimates of the probability of neurotransmitter release (*P*r) and quantal amplitude in both cortical and thalamic inputs in control and mutant mice. First, we compared the rate of the progressive block of the isolated NMDA (N-methyl-D-aspartate) receptor-mediated EPSC in slices by the irreversible open-channel blocker of the NMDA receptor channel, MK-801 (40μM). In the presence of MK-801, the rate of decline of the NMDAR EPSC in the course of repetitive presynaptic stimulation is determined by *P*r at stimulated synapses (NMDAR channels are blocked by MK-801 when they are opened by synaptically-released glutamate; Figure 4; Shin et al., 2006). Second, we measured the amplitude of synaptic events evoked by presynaptic stimulation in both cortical and thalamic projections to the LA, when bath Sr^{2+} was substituted for Ca^{2+}. Under such conditions, presynaptic pulses evoke asynchronous single-quantum EPSCs in the stimulated pathway, which could be observed for several hundred ms after the stimulus. We did not observe significant differences between control and mutant animals in *P*r or quantal amplitude, either at cortico-amygdala (Figure 4A–D and Figure S9) or thalamo-amygdala synapses (Figure 4E–H and Figure S9). Together, these findings indicate that deletion of TRPC5 had no detectable effect on the firing properties of LA neurons and basal synaptic transmission in afferent inputs to the LA in 4–5 week-old mice.

We also investigated the role of TRPC5 in synaptic transmission at excitatory inputs to intercalated cells (Royer et al., 2000). Residing in a narrow strip of cellular clusters between the BLA complex and the central nucleus of the amygdala (CeA), they receive synaptic inputs from the lateral and basal nuclei and project to the CeA. Intercalated neurons control the level of neuronal activity in the CeA by releasing the inhibitory neurotransmitter, GABA, onto CeA neurons, thus contributing to fear-related behavioral responses (Pare et al., 2004). We stimulated neurons in the LA and recorded EPSCs in intercalated cells. We did not observe any differences between control and *TRPC5*$^{-/-}$ mice in synaptic input-output curves (Figure S10A), the magnitude of paired-pulse facilitation (Figure S10B), or in the amplitude and frequency of spontaneous glutamatergic EPSCs (sEPSCs; Figure S10C,D). Thus basal synaptic transmission in inputs to intercalated cells was normal in TRPC5$^{-/-}$ mice.

Long-term potentiation (LTP) in CS pathways may contribute to the acquisition of fear memory in response to auditory stimulation (Rogan et al., 1997; Tsvetkov et al., 2002). As shown in Figure 1, TRPC5 is expressed in the LA and areas of the auditory cortex implicated in fear conditioning. We examined LTP of the excitatory postsynaptic potentials (EPSPs) in cortical and thalamic inputs to the LA in slices from 4–5 week-old mice. The magnitude of spike timing-

dependent LTP (Bi and Rubin, 2005; Shin et al., 2006), induced in the presence of the $GABA_A$-receptor antagonist picrotoxin (50 μM), was not different between experimental groups. Cortico-amygdala EPSPs were potentiated to 127±7% in control mice and to 129±5% of the baseline amplitude in *TRPC5*$^{-/-}$ mice (Figure 3E,F). In thalamic input to the LA, EPSPs were potentiated to 135±19% in control mice and to 132±8% in *TRPC5*$^{-/-}$ mice (Figure 3H, **I**). Thus, TRPC5 was not required for spike timing-dependent LTP in afferent inputs to the amygdala.

Reduced Group I mGluR and CCK_2 Receptor-Mediated Currents in TRPC5$^{-/-}$ LA Neurons

Recent studies suggest that activation of $G_{q/11}$ protein-coupled receptors (*e.g.* mGluRs and cholecystokinin$_2$ (CCK_2) receptors) in the amygdala may lead to the opening of heteromultimeric TRP channels containing the TRPC5 subunit (Faber et al., 2006; Meis et al., 2007). Moreover, pharmacological block of Group I mGluRs (mGluR1 and mGluR5 subtypes) in the amygdala diminished both innate (Perez de la Mora et al., 2006; Pietraszek et al., 2005) and learned fear responses (Rodrigues et al., 2002). Additionally, blockade of CCK_2 receptors, which are activated by endogenously released CCK in response to anxiety (innate fear) provoking stimuli, is associated with distinctive anxiolytic effects (Frankland et al., 1997; Wang et al., 2005). We thus investigated whether mGluR- and/or CCK_2-mediated synaptic responses in the LA were affected by ablation of the *TRPC5* gene.

Delivery of short trains of high frequency stimulation (10 pulses at 100 Hz) to either the cortico-amygdala or thalamo-anygdala fibers resulted in large, prolonged EPSPs in LA neurons (Figure 5A,B,C). The size of synaptic responses was significantly decreased by block of AMPA, NMDA, and GABA receptors. The residual component of the EPSP, presumably mediated by synaptic activation of mGluRs (Faber et al., 2006), was significantly smaller in slices from *TRPC5*$^{-/-}$ mice, both in cortico-amygdala (Figure 5C, $P<0.04$) and in thalamo-amygdala pathways (Figure 5C, $P<0.05$). To further characterize mGluR-mediated synaptic responses, we recorded EPSCs evoked over −100 mV to +40mV in the presence of AMPA, NMDA, $GABA_B$ and $GABA_A$ receptor blockers. The current-voltage (I–V) relation of the peak EPSC was similar in both experimental groups. The EPSC amplitude, however, was consistently smaller in slices from null mice at all holding potentials tested (Figure 5D,E). In agreement with previous reports (Faber et al., 2006), both mGluR1 and mGluR5 receptors were recruited by synaptically-released glutamate in slices from control mice. This is evidenced by the high sensitivity of the EPSCs at a holding potential of +40 mV to the specific mGluR5 and mGluR1 antagonists, MPEP and CPCCOEt, respectively (Figure 5G–I).

The I–V curve for mGluR-mediated synaptic currents in slices from control mice, recorded in inputs to the LA in the presence of the mGluR5 antagonist MPEP, was very similar to the I–V relation for same-synaptic responses recorded in slices from TRPC5 null mice (Figure 5F). This supports the notion that synaptic activation of Group I mGluRs results in the opening of TRPC5 channels in control animals (Faber et al., 2006). The blocking effect of simultaneously applied MPEP and CPCCOEt did not differ from their individual effects (Figure 5I) indicating the lack of additivity in the action of these antagonists. The residual component of the synaptically induced mGluR-mediated current, observed in the presence of MPEP and CPCCOEt, was largely mediated by Group III mGluRs since it was reduced to 10±3% of the baseline amplitude in the presence of the Group III antagonist UBP1112 (30μM). Consistent with the role of the mGluR-mediated synaptic responses in control of neuronal spike firing (which could reflect incoming afferent activity), we found that the number of extracellular spikes (Otmakhov et al., 1993) evoked in individual LA neurons by presynaptic pulses of increasing intensity (Figure 6A–D) was significantly decreased in slices from TRPC5 null mice for both cortical (Figure 6C,E,) and thalamic (Figure 6D,F) inputs.

Finally, we recorded membrane currents induced in LA neurons by the specific agonist of CCK_2 receptors, cholecystokinin 4 (CCK4, 3μM), in slices from 4–5 week old control (Figure 7A,E) and *TRPC5*$^{-/-}$ mice (Figure 7E). In control slices, addition of CCK4 to the external solution evoked inward currents in all LA neurons tested (Figure 7B). This current was completely eliminated by 2-APB (100μM), a nonselective TRP channel blocker (Clapham, 2007; Figure 7C). Consistent with the intracellular Ca^{2+} sensitivity of TRPC5-containing channel complexes (Strübing et al., 2001), CCK4-induced currents at −70mV were largely blocked when intracellular free [Ca^{2+}] was buffered to <10nM by inclusion of 10mM BAPTA in the pipette (n=15 cells, $P<0.001$). Responses to CCK4 were significantly diminished in slices from *TRPC5*$^{-/-}$ mice (Figure 7D–F). We found that the ability of exogenously-applied CCK to increase spike firing in response to depolarizing current injections was significantly diminished in slices from TRPC5 null mice (Figure 7G,H,I), which would result in the decreased firing output of neurons in the amygdala. We conclude that the deficits in fear-related behaviors in mutant mice result, in part, from the lack of TRPC5 activation through Group I mGluRs- and/or neuropeptide CCK-linked pathways.

DISCUSSION

Our results provide direct evidence that TRPC5 is involved in the control of fear-related behaviors, both learned and innate. In blinded behavioral studies, mice lacking TRPC5 were significantly less anxious in response to innately aversive stimuli than their *wt* littermates. In addition, TRPC5 may contribute to conditioned (learned) fear under certain conditions. We hypothesize that the changes in fear behavior were due to abrogation of CCK_2 and/or glutamate-mediated potentiation of TRPC5 currents.

TRPC5 is present in pyramidal neurons in the auditory cortex, the S1/S2 areas of the somatosensory cortex, and the parietal insular cortex that supply sensory input to the amygdala. TRPC5 is also present in the hippocampus and dentate gyrus that project to the amygdala, and in the perirhinal cortex (PRh) that relays CS and somatosensory US information (Lanuza et al., 2004; LeDoux, 2000; Shi and Davis, 1999; Shumyatsky et al., 2005). Our findings show that responses to the CCK_2 receptor agonist, and cortico-amygdala EPSPs, mediated by Group I mGluRs, were significantly diminished in slices from *TRPC5*$^{-/-}$ mice, while basal synaptic transmission in cortical and thalamic inputs to the LA and inputs from the LA to intercalated cells (Pare et al., 2004) was unaltered. Thus, deficits in fear-related behaviors may result from the lack of TRPC5 activation or potentiation by Group I mGluRs- and/or neuropeptide cholecystokinin-linked pathways.

The contribution of TRPC5 to synaptic function might be greater at earlier developmental stages, as basal synaptic transmission at cortical inputs was found to be impaired in slices from P10-P13 *TRPC5*$^{-/-}$ mice. Normal basal synaptic transmission in older mutant mice could reflect the ~2-fold decrease at 4–5 weeks compared to P10 mice. Most important, responses mediated by activation of $G_{q/11}$ protein-coupled receptors were impaired in neurons of 4–5 week-old *TRPC5*$^{-/-}$ mice.

Synaptic activation of Group I mGluRs or activation of CCK_2 receptors in the amygdala was shown to have anxiogenic effects (Pietraszek et al., 2005; Wang et al., 2005). As observed in our study in *TRPC5*$^{-/-}$ mice, the inability of CCK to produce membrane depolarization and the decreased mGluR-mediated EPSPs could diminish the firing output of neurons in brain circuits underlying innate fear reactions. This would result from the decreased probability of spike firing (Meis et al., 2007) in response to synaptic activation, thus preventing transmission of specific signals, afferent or innate, to other components of the innate fear circuitry, and provide a mechanistic explanation for the anxiolytic-like behavioral phenotype in TRPC5$^{-/-}$ mice.

The observation that conditioned fear memory, as assessed with the single-trial fear conditioning training paradigm, was not affected in TRPC5$^{-/-}$ mice is consistent with the lack of change in spike timing-dependent LTP in the CS pathways (cortical and thalamic inputs to the LA). Since conditioned freezing was enhanced in mutant mice following multiple CS-US pairings, TRPC5 may contribute to conditioned fear under certain training conditions. Although LTP in the CS pathways was not affected by TRPC5 ablation, more pronounced decreases in spiking output of neurons in the BLA complex to their targets, such as intercalated cells, during the CS presentation following multiple CS-US pairings (as opposed to a single pairing) could result in decreased inhibition of neurons in the CeA, thus leading to the enhanced fear responses in conditioned animals (Pare et al., 2004). Alternatively, repeated US presentations could paradoxically produce enhancement of innate fear in TRPC5$^{-/-}$ mice, manifested as enhanced freezing in response to the CS presentation while, in fact, fear memory was not affected.

Recent findings indicate that brain region and neural circuitry-specific gene expression may determine different aspects of fear-related behaviors (Shumyatsky et al., 2002; 2005). Thus, the phosphoprotein stathmin, which is found in principal neurons where it contributes to microtubule dynamics and is necessary for TRPC5 transit in neurites (Greka et al, 2003), is highly expressed in areas controlling both learned and innate fear responses. Stathmin null mice showed deficits in both innate and conditioned fear (Shumyatsky et al., 2005). In the present study, we found that TRPC5, possibly acting in concert with intracellular pathways implicating stathmin, also contributes to both conditioned freezing and innate fear. Our finding that LTP in cortical and thalamic inputs to the LA was not affected in *TRPC5* null mice provides an interesting example in which deletion of a single gene had an effect on conditioned (following multiple CS-US pairings) and innate fear without changes in LTP in the CS pathway. Considered together, our findings provide further support to the view that behavioral responses can be driven by neural circuitry-specific gene expression (Rodrigues et al., 2004; Shumyatsky et al., 2005).

We found that only one of the two auditory CS areas, the auditory cortex, contains TRPC5. Cortico-amygdala and thalamo-amygdala projections could have different roles in both encoding fear memory and triggering learned and innate fear responses (Doyere et al., 2003). Thus, it has been suggested that the auditory cortex might contribute to CS discrimination, processing complex patterned tones (Armony et al., 1997). The lack of TRPC5 expression in the auditory thalamus implies that the TRPC5 expression pattern may determine directionality of the information flow in brain networks underlying fear related behaviors. Although basal synaptic transmission in cortical input to the LA was normal in juvenile *TRPC5* null mice, cortically expressed TRPC5 could control the efficacy of afferent inputs received by the auditory cortex. This would determine whether the signal is transmitted from the auditory cortex to other brain regions implicated in fear behavior. Therefore, it will be important to correlate expression patterns of TRPC5 with Gαq-linked receptors such as mGluRs and CCK2.

EXPERIMENTAL PROCEDURES

Generation of *TRPC5*$^{-/-}$ mice

TRPC5$^{-/-}$ mice were generated by recombineering (Liu et al., 2003). Material for homologous recombination was provided by the NCI-Frederick Institute (http://recombineering.ncifcrf.gov/). Chimeric mice were generated by injection of the ES cells into C57BL/6 mouse blastocysts. The chimeric mice were bred with 129/SvImJ mice. Tail genomic DNA contained the TRPC5 mutation in agouti offspring. The F2 heterozygous mice were backcrossed to 129/SvImJ mice for eight generations. Heterozygotes were then crossed to generate paired littermates for all studies.

RT-PCR analysis

Total RNA was isolated from whole brain of control and *TRPC5*$^{-/-}$ littermates using TRIzol (Invitrogen; see Supplemental Data). For quantitative RT-PCR, the amygdala was dissected from 0.6 mm brain sections obtained from six 4.5 week-old and six 15-day old mice. PCR primers for mouse *TRPC1*, *TRPC4*, *TRPC5*, *TRPC6*, *TRPC7* and *β-actin* were added to SYBR Green 2x Mastermix (Applied Biosystems,) to a final concentration of 300 nM. QRT-PCR was carried out as described previously (Riccio et al., 2002).

In situ hybridization

Brains were isolated from 4 week-old mice and frozen in powdered dry ice. Cryostat sections (18–20μm) were hybridized with a digoxygenin cRNA probe generated by *in vitro* transcription (Roche). After color development, slides were incubated with mouse monoclonal to CaMKII (1:200, Abcam) followed by incubation with goat anti-mouse Alexafluor-488 fluorescent secondary antibody (1:200, Molecular Probes) for double labeling.

Immunoprecipitation and Immunohistochemistry

Brain microsomes (4 wk mouse) were solubilized in IP buffer; 1mg was IP'd with 5μg anti-TRPC5 antibody (NeuroMab, UC Davis) and 10μg protein A sepharose (Amersham Pharmacia). Antibodies for western blots: 5μg/ml anti-TRPC5 and anti-Na^+, K^+-ATPase-α (NKA-α) (1:5000; Axxora); 1:10,000 dilution of secondary goat anti-mouse IgG light chain conjugated with HRP (Jackson ImmunoResearch) or secondary goat anti-rabbit IgG conjugated with HRP (Pierce) for 1h at 22°C. 4um formalin-fixed, paraffin-embedded tissue sections were immunostained (see Supplemental Experimental Procedures).

Electrophysiological recordings

Control or *TRPC5*$^{-/-}$ mice (littermates) amygdalae were vibratome-sliced into 250–300μm sections. Whole-cell recordings of evoked EPSCs were obtained from pyramidal neurons in the lateral amygdala under visual guidance (DIC/infrared optics). Slices were continuously superfused in solution containing (in mM): 119 NaCl, 2.5 KCl, 2.5 $CaCl_2$, 1.0 $MgSO_4$, 1.25 NaH_2PO_4, 26.0 $NaHCO_3$, 10 glucose, and 0.1 picrotoxin and equilibrated with 95% O_2 and 5% CO_2 (pH 7.3–7.4) at 22°C. Cells were classified as principal neurons by their appearance and spike frequency adaptation to prolonged depolarizing current injection (Tsvetkov et al., 2002). Patch electrodes (3–5 MΩ) in current-clamp experiments contained (in mM): 120 K-gluconate, 5 NaCl, 1 $MgCl_2$, 0.2 EGTA, 10 HEPES, 2 MgATP, and 0.1 NaGTP (adjusted to pH 7.2 with KOH). In voltage-clamp experiments, 120mM Cs-methane-sulfonate replaced K-gluconate. Free [Ca^{2+}] was buffered to ~100nM in CCK4 experiments with 5mM EGTA/ 1.97mM $CaCl_2$ in the pipette solution. Synaptic responses were evoked by stimulation of fibers in the external capsule (cortical input) or the internal capsule (thalamic input) by a concentric stimulating electrode (Shin et al., 2006; Tsvetkov et al., 2002). Currents were filtered at 1kHz and digitized at 5kHz. EPSC amplitudes = I_{avg} in a 1–2ms window at peak minus I_{avg} during prestimulus baseline. LTP was induced with 80 presynaptic stimuli delivered at 2Hz to the cortical or thalamic inputs, paired with action potentials evoked in a postsynaptic cell with 4–8ms delay from the onset of each EPSP (Shin et al., 2006). Summary LTP graphs were constructed by normalizing data in 60 s epochs to the mean value of the baseline EPSP. Spontaneous mEPSCs were analysed using Mini Analysis (Synaptosoft Inc).

Behavioral assays

All behavioral tests were conducted with counterbalanced groups (wild type and null mice; male adults); the experimenters were blind to genotype in all electrophysiological and behavioral studies. All experimental procedures, including elevated plus maze, open field, acoustic startle, social interaction test, novelty-suppressed feeding, locomotor activity, and

auditory fear conditioning, were approved by the McLean Hospital's IACUC. Details of each behavioral test are provided in the Supplementary Experimental Procedures.

Supplementary Material

Refer to Web version on PubMed Central for supplementary material.

Acknowledgments

We thank Lin Lin Zhao for her help with maintaining the TRPC5 mouse colony and Kenneth Law for help with immunostaining. We also thank the Gene Manipulation Facility of the Children's Hospital Mental Retardation and Developmental Disabilities Research Center (grant NIH P30-HD18655). This work was supported by grants from the National Institutes of Health, NARSAD, and the Whitehall Foundation (V.Y.B).

References

Armony JL, Servan-Schreiber D, Romanski LM, Cohen JD, LeDoux JE. Stimulus generalization of fear responses: effects of auditory cortex lesions in a computational model and in rats. Cereb Cortex 1997;7:157–165. [PubMed: 9087823]

Bezzerides VJ, Ramsey IS, Kotecha S, Greka A, Clapham DE. Rapid vesicular translocation and insertion of TRP channels. Nat Cell Biol 2004;6:709–720. [PubMed: 15258588]

Bi GQ, Rubin J. Timing in synaptic plasticity: from detection to integration. Trends Neurosci 2005;28:222–228. [PubMed: 15866196]

Bissiere S, Humeau Y, Luthi A. Dopamine gates LTP induction in lateral amygdala by suppressing feedforward inhibition. Nat Neurosci 2003;6:587–592. [PubMed: 12740581]

Clapham DE. TRP channels as cellular sensors. Nature 2003;426:517–524. [PubMed: 14654832]

Clapham DE. SnapShot: mammalian TRP channels. Cell 2007;129:220. [PubMed: 17418797]

Davis M, Whalen PJ. The amygdala: vigilance and emotion. Mol Psychiatry 2001;6:13–34. [PubMed: 11244481]

Doyere V, Schafe GE, Sigurdsson T, LeDoux JE. Long-term potentiation in freely moving rats reveals asymmetries in thalamic and cortical inputs to the lateral amygdala. Eur J Neurosci 2003;17:2703–2715. [PubMed: 12823477]

Faber ES, Sedlak P, Vidovic M, Sah P. Synaptic activation of transient receptor potential channels by metabotropic glutamate receptors in the lateral amygdala. Neuroscience 2006;137:781–794. [PubMed: 16289832]

Fanselow MS, LeDoux JE. Why we think plasticity underlying Pavlovian fear conditioning occurs in the basolateral amygdala. Neuron 1999;23:229–232. [PubMed: 10399930]

Fanselow MS, Poulos AM. The neuroscience of mammalian associative learning. Annu Rev Psychol 2005;56:207–234. [PubMed: 15709934]

Frankland PW, Josselyn SA, Bradwejn J, Vaccarino FJ, Yeomans JS. Activation of amygdala cholecystokininB receptors potentiates the acoustic startle response in the rat. J Neurosci 1997;17:1838–1847. [PubMed: 9030642]

Gordon JA, Hen R. Genetic approaches to the study of anxiety. Annu Rev Neurosci 2004;27:193–222. [PubMed: 15217331]

Greka A, Navarro B, Oancea E, Duggan A, Clapham DE. TRPC5 is a regulator of hippocampal neurite length and growth cone morphology. Nat Neurosci 2003;6:837–845. [PubMed: 12858178]

Kodirov SA, Takizawa S, Joseph J, Kandel ER, Shumyatsky GP, Bolshakov VY. Synaptically released zinc gates long-term-potentiation in fear conditioning pathways. Proc Natl Acad Sci USA 2006;103:15218–15223. [PubMed: 17005717]

Lanuza E, Nader K, Ledoux JE. Unconditioned stimulus pathways to the amygdala: effects of posterior thalamic and cortical lesions on fear conditioning. Neuroscience 2004;125:305–315. [PubMed: 15062974]

LeDoux JE. Emotion circuits in the brain. Annu Rev Neurosci 2000;23:155–184. [PubMed: 10845062]

Liu P, Jenkins NA, Copeland NG. A highly efficient recombineering-based method for generating conditional knockout mutations. Genome Res 2003;13:476–484. [PubMed: 12618378]

Maren S, Quirk GJ. Neuronal signalling of fear memory. Nat Rev Neurosci 2004;5:844–852. [PubMed: 15496862]

McGaugh JL. Memory – a century of consolidation. Science 2000;287:248–251. [PubMed: 10634773]

McKernan MG, Shinnick-Gallagher P. Fear conditioning induces a lasting potentiation of synaptic currents in vitro. Nature 1997;390:607–611. [PubMed: 9403689]

Meis S, Munsch T, Sosulina L, Pape HC. Postsynaptic mechanisms underlying responsiveness of amygdaloid neurons to cholecystokinin are mediated by a transient receptor potential-like current. Mol Cell Neurosci 2007;35:356–367. [PubMed: 17482476]

Milad MR, Rauch SL, Pitman RK, Quirk GJ. Fear extinction in rats: implications for human brain imaging and anxiety disorders. Biol Psychol 2006;73:61–71. [PubMed: 16476517]

Otmakhov N, Shirke AM, Malinow R. Measuring the impact of probabilistic transmission on neuronal output. Neuron 1993;10:1101–1111. [PubMed: 8318231]

Pare D, Quirk GP, LeDoux JE. New vistas on amygdala networks in conditioned fear. J Neurophysiol 2004;92:1–9. [PubMed: 15212433]

Perez de la Mora M, Lara-Garcia D, Jacobsen KX, Vazquez-Garcia M, Crespo-Ramirez M, Flores-Gracia C, Escamilla-Marvan E, Fuxe K. Anxiolytic-like effects of the selective metabotropic glutamate receptor 5 antagonist MPEP after its intra-amygdaloid microinjection in three different non-conditioned rat models of anxiety. Eur J Neurosci 2006;23:2749–2759. [PubMed: 16817878]

Pietraszek M, Sukhanov I, Maciejak P, Szyndler J, Gravius A, Wislowska A, Plaznik A, Bespalov AY, Danysz W. Anxiolytic-like effects of mGlu1 and mGlu5 receptor antagonists in rats. Eur J Pharmacol 2005;514:25–34. [PubMed: 15878321]

Pitkanen A, Savander V, LeDoux JE. Organization of intra-amygdaloid circuitries in the rat: an emerging framework for understanding functions of the amygdala. Trends Neurosci 1997;20:517–523. [PubMed: 9364666]

Ramsey IS, Moran MM, Chong JA, Clapham DE. A voltage-gated proton-selective channel lacking the pore domain. Nature 2006;440:1213–1216. [PubMed: 16554753]

Riccio A, Mattei C, Kelsell RE, Medhurst AD, Calver AR, Randall AD, Davis JB, Benham CD, Pangalos MN. Cloning and functional expression of human short TRP7, a candidate protein for store-operated Ca2+ influx. J Biol Chem 2002;277:12302–12309. [PubMed: 11805119]

Rodrigues SM, Bauer EP, Farb CR, Schafe GE, LeDoux JE. The group I metabotropic glutamate receptor mGluR5 is required for fear memory formation and long-term potentiation in the lateral amygdala. J Neurosci 2002;22:5219–5229. [PubMed: 12077217]

Rodrigues SM, Schafe GE, LeDoux JE. Molecular mechanisms underlying emotional learning and memory in the lateral amygdala. Neuron 2004;44:75–91. [PubMed: 15450161]

Rogan MT, Staubli UV, LeDoux JE. Fear conditioning induces associative long-term potentiation in the amygdala. Nature 1997;390:604–607. [PubMed: 9403688]

Royer S, Martina M, Pare D. Polarized synaptic interactions between intercalated neurons of the amygdala. J Neurophysiol 2000;83:3509–3518. [PubMed: 10848566]

Seidenbecher T, Laxmi TR, Stork O, Pape HC. Amygdalar and hippocampal theta rhythm synchronization during fear memory retrieval. Science 2003;301:846–850. [PubMed: 12907806]

Shi C, Davis M. Pain pathways involved in fear conditioning measured with fear-potentiated startle: lesion studies. J Neurosci 1999;19:420–430. [PubMed: 9870970]

Shim S, Goh EL, Ge S, Sailor K, Yuan JP, Roderick HL, Bootman MD, Worley PF, Song H, Ming GL. XTRPC1-dependent chemotropic guidance of neuronal growth cones. Nat Neurosci 2005;8:730–735. [PubMed: 15880110]

Shin RM, Tsvetkov E, Bolshakov VY. Spatiotemporal asymmetry of associative synaptic plasticity in fear conditioning pathways. Neuron 2006;52:883–896. [PubMed: 17145508]

Shumyatsky GP, Tsvetkov E, Malleret G, Vronskaya S, Hatton M, Hampton L, Battey JF, Dulac C, Kandel ER, Bolshakov VY. Identification of a signaling network in lateral nucleus of amygdala important for inhibiting memory specifically related to learned fear. Cell 2002;111:905–918. [PubMed: 12526815]

Shumyatsky GP, Malleret G, Shin RM, Takizawa S, Tully K, Tsvetkov E, Zakharenko SS, Joseph J, Vronskaya S, Yin D, et al. Stathmin, a gene enriched in the amygdala, controls both learned and innate fear. Cell 2005;123:697–709. [PubMed: 16286011]

Strübing C, Krapivinsky G, Krapivinsky L, Clapham DE. TRPC1 and TRPC5 form a novel cation channel in mammalian brain. Neuron 2001;29:645–655. [PubMed: 11301024]

Tsvetkov E, Carlezon WA, Benes FM, Kandel ER, Bolshakov VY. Fear conditioning occludes LTP-induced presynaptic enhancement of synaptic transmission in the cortical pathway to the lateral amygdala. Neuron 2002;34:289–300. [PubMed: 11970870]

Tsvetkov E, Shin RM, Bolshakov VY. Glutamate uptake determines pathway specificity of long-term potentiation in the neural circuitry of fear conditioning. Neuron 2004;41:139–151. [PubMed: 14715141]

Wang GX, Poo MM. Requirement of TRPC channels in netrin-1-induced chemotropic turning of nerve growth cones. Nature 2005;434:898–904. [PubMed: 15758951]

Wang H, Wong PT, Spiess J, Zhu YZ. Cholecystokinin-2 (CCK2) receptor-mediated anxiety-like behaviors in rats. Neurosci Biobehav Rev 2005;29:1361–1373. [PubMed: 16120463]

Zucker RS, Regehr WG. Short-term synaptic plasticity. Annu Rev Physiol 2002;64:355–405. [PubMed: 11826273]

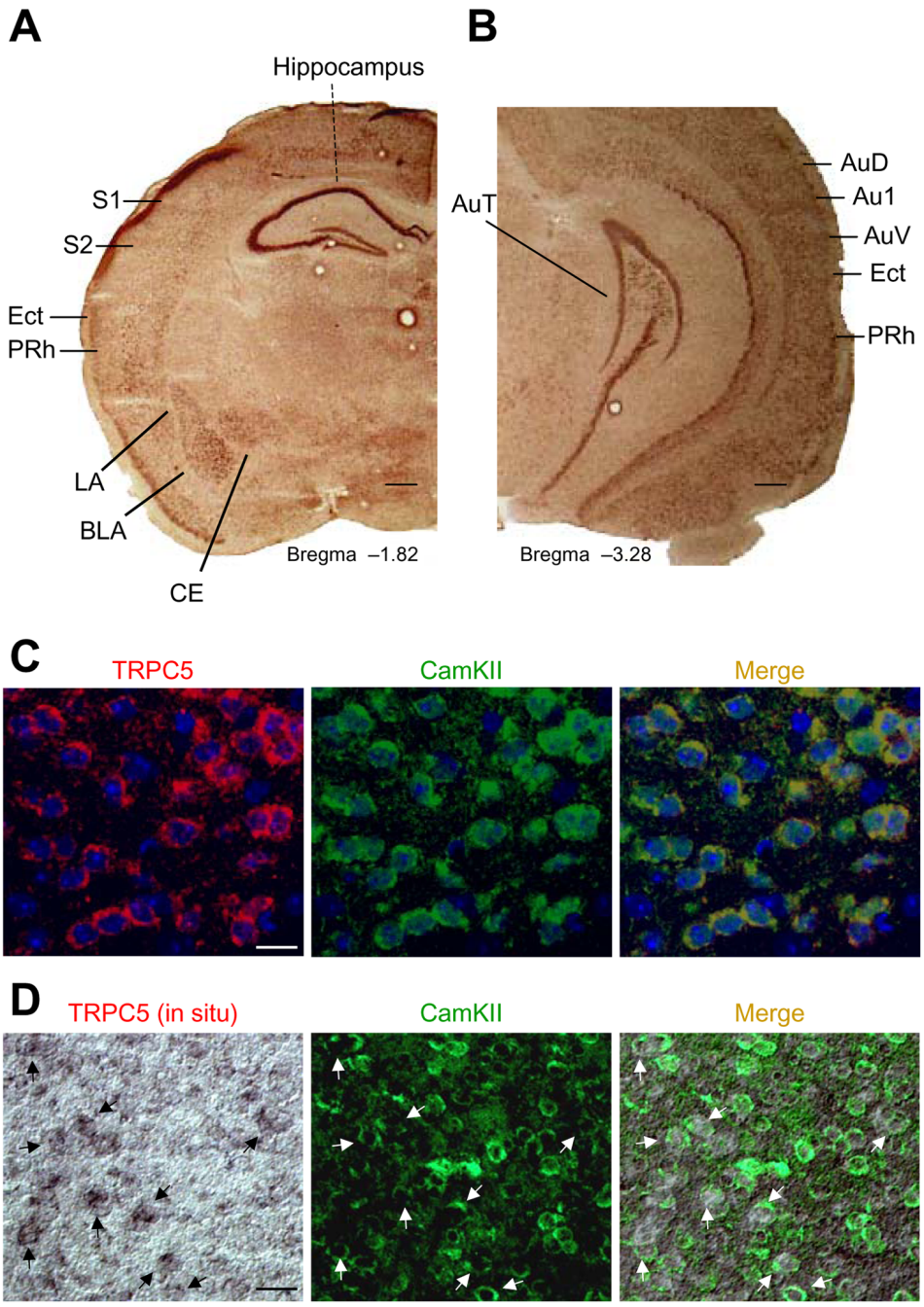

Figure 1. TRPC5 distribution in mouse brain

(A, B) *In situ* hybridization of TRPC5-mRNA in the amygdala, hippocampus, somatosensory cortex, and auditory cortex. LA, lateral nucleus of the amygdala; BLA, basolateral nucleus of the amygdala; CE central nucleus of the amygdala; S1, primary somatosensory cortex; S2, secondary somatosensory cortex; AuD, secondary auditory cortex, dorsal; Au1, primary auditory cortex; AuV, secondary auditory cortex, ventral; Ect, ectorhinal cortex; PRh, perirhinal cortex. Scale bar, 1mm. **(C),** TRPC5 (left) and CaMKIIα (middle, a marker of pyramidal neurons) colocalize in the lateral nucleus of the amygdala. Scale bar, 25 μm. **(D)** TRPC5 (left, *in situ* hybridization) and anti-CaMKIIα (middle) co-localize in the majority of

pyramidal cells of the auditory cortex. Arrows indicate cells expressing both TRPC5 and CaMKIIα. Scale bar, 50 μm.

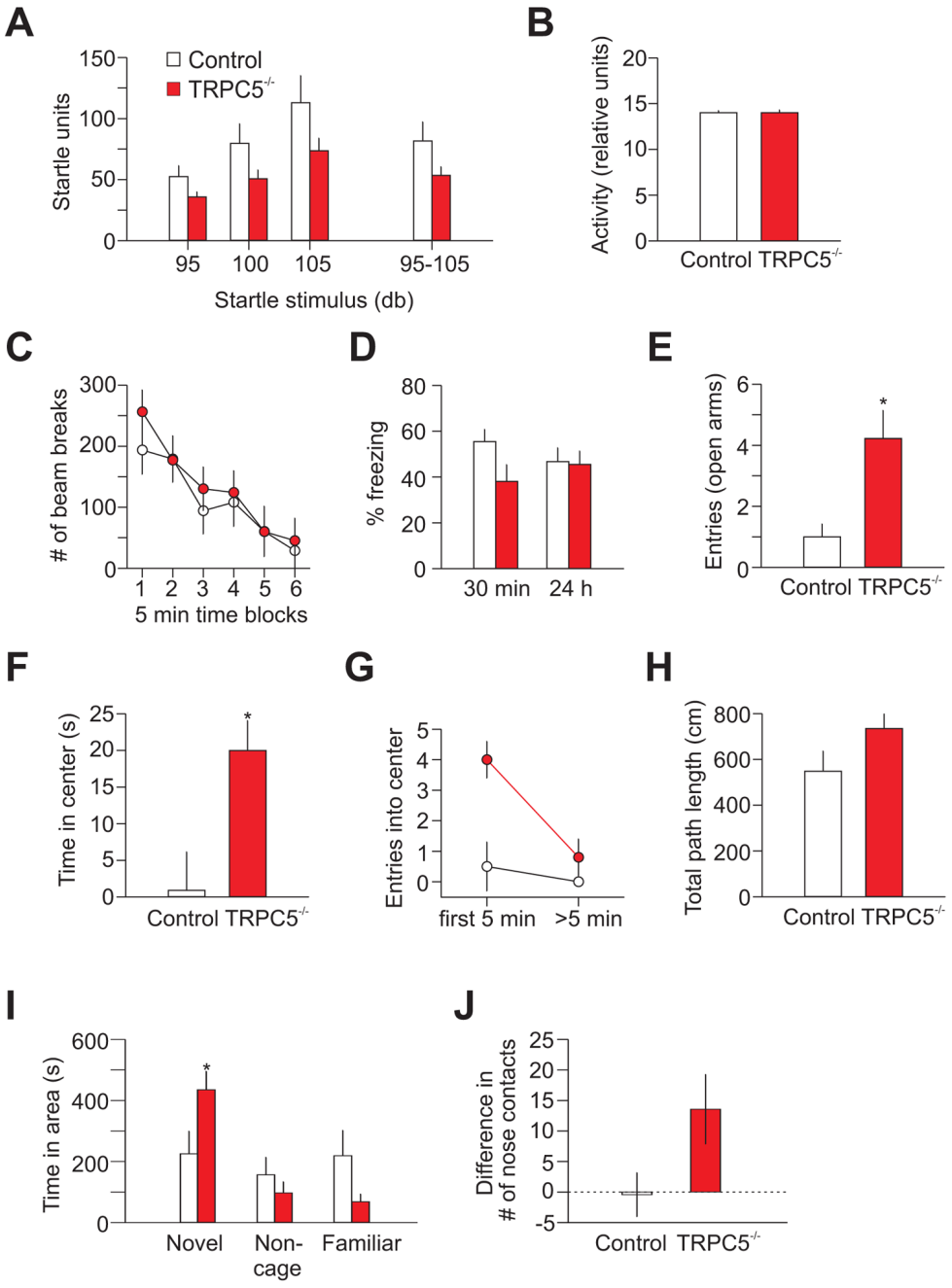

Figure 2. Mice lacking TRPC5 display an anxiolytic-like phenotype

(A) The acoustic startle response to auditory stimuli at 95, 100 and 105dB in control (n=10; white) and null (n=9; red) mice. ANOVA, F(1,17)=2.9, *P*=0.1. **(B)** Activity levels in control and null mice sampled immediately preceding the onset of the startle stimuli for the experiments shown in (A). **(C)** Locomotor activity of *TRPC5*$^{-/-}$ and *wt* mice were indistinguishable (8 mice per group; *P*=0.7). **(D)** Conditioned 'freezing' following single-trial fear conditioning in control mice (n=10) and *TRPC5*$^{-/-}$ mice (n=10) at 30min (ANOVA, *P*=0.054) and 24h (ANOVA, F(1,18) = 0.02, *P*=0.9) post-training. **(E)** Elevated plus-maze experiments: *TRPC5*$^{-/-}$ mice entered the open arm of the maze more commonly (10 mice per group; open arms: $t_{(18)}$=2.75, *P*<0.05; closed arms $t_{(18)}$=1.44, *P*=0.17, not shown). **(F–H)** In open field

experiments, *TRPC5*$^{-/-}$ mice spent more time in the center of the arena [F(1,14)=5.16, *P*=0.04] (**F**) and (**G**) entered it more frequently [F(1,14)=5.6, *P*=0.03]; ≤5 min versus >5 min [F(1,14) =7.0, *P*=0.02]. Total path length did not differ between groups (**H**) Total path lengths; [F(1,14) =2.7, *P*=0.1]; 8 mice per group). **(I, J)** Social interaction test; (**I**) Duration of time spent by mice of both genotypes in each of the 3 areas of the testing apparatus during the preference for social novelty phase (7 mice per group). Mutant mice spent more time with the novel mouse (t test, t=2.2, *P*=0.04); (**J**) Average difference between the number of nose contacts with the novel and familiar mouse. Error bars indicate SEM.

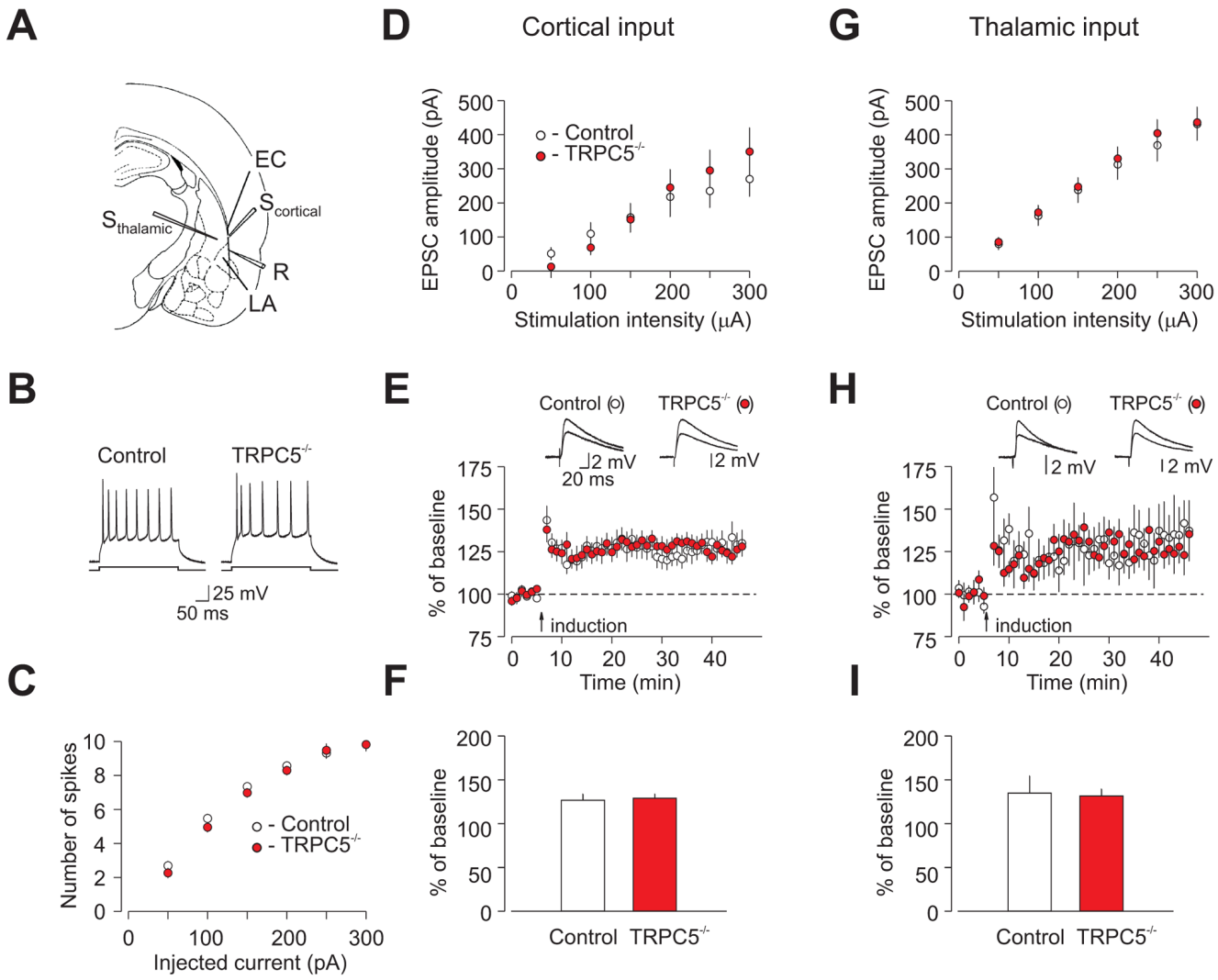

Figure 3. Membrane excitability and synaptic function in the LA are normal in 4–5 week-old *TRPC5*$^{-/-}$ mice

(A) Position of the stimulation ($S_{thalamic}$, $S_{cortical}$) and recording (R) electrodes. EC, external capsule. **(B)** Responses of LA neurons to current injection (150 pA) recorded in current-clamp mode. **(C)** Summary plots of the number of spikes in LA neurons evoked by current injection of increasing intensity in slices from control (open symbols) and *TRPC5*$^{-/-}$ (filled symbols) mice, recorded as in (B). From 4 wt mice, n=32 neurons, and 5 null mice, n=39 neurons. ANOVA, *P*=0.75 **(D)** Synaptic input-output curves obtained in the cortical input to the LA. Cortico-amygdala EPSCs were recorded under voltage-clamp conditions (V_H=−70 mV). EPSC amplitude is plotted vs. stimulation intensity (*wt* mice, n=14 neurons; null mice, n = 10 neurons. ANOVA, *P*=0.7 **(E)** Action potential-EPSP pairing-induced LTP of the cortico-amygdala EPSP recorded in the LA neuron in slices. Insets show the average of 10 EPSPs recorded before, and 35min after, the induction (arrow). **(F)** Summary of LTP experiments at cortico-amygdala synapses (from 7 *wt* mice, n=20 neurons, and 7 null mice, n=19 neurons) t test, *P*=0.8. **(G)** Synaptic input-output curves obtained in the thalamic input to the LA (from 4 *wt* mice, n=22 neurons, and 5 null mice, n=24 neurons; ANOVA, *P*=0.8. **(H)** LTP of the thalamo-amygdala EPSP recorded in the LA neuron. Insets show the average of 10 EPSPs recorded before, and 35min after, the induction (arrow). **(I)** Summary of LTP experiments at the thalamo-amygdala

synapses (from 5 *wt* mice, n=8 neurons, and 5 null mice, n=10 neurons; t test, P=0.87. Error bars indicate SEM.

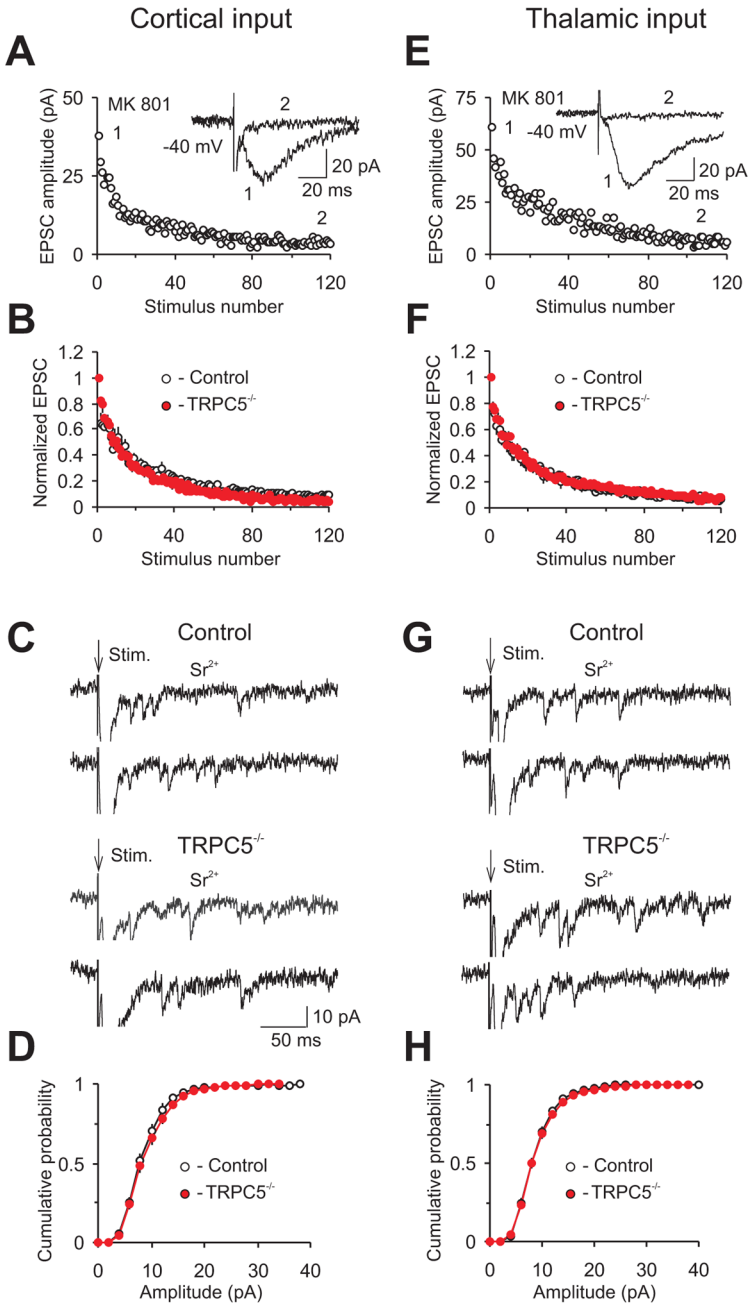

Figure 4. Quantal parameters of synaptic transmission at cortical and thalamic inputs to the LA are normal in TRPC5$^{-/-}$ mice

(A) Progressive block by MK-801 (40μM) of the NMDA receptor EPSC recorded in cortical input to the LA in the presence of CNQX (20μM; V_H=−40 mV). MK-801 was applied to the slice in the absence of presynaptic stimulation for >10min and the external capsule was then stimulated at 0.1Hz to measure the rate of MK-801 block. Inset shows the baseline NMDAR EPSC (1) and its block at the end of presynaptic stimulation in the presence of MK-801 (2). **(B)** Summary graphs of the experiments with MK-801 protocol in cortical input (as in A). In each individual experiment, EPSC amplitudes were normalized by the first EPSC (from 3 *wt* mice, n=7 neurons and 4 *TRPC5* null mice, n=10 neurons; ANOVA, *P*=0.9). **(C)**

Representative traces of the asynchronous quantal EPSCs evoked by stimulation (at arrow) of the cortical input (V_H= −70 mV). In these experiments, Sr2+ was substituted for extracellular Ca^{2+}. **(D)** Cumulative amplitude histograms of asynchronous quantal events recorded in the cortical input to the LA (from 3 *wt* mice, n=11 neurons and 4 *TRPC5* null mice, n=17 neurons). **(E)** Progressive block by MK-801 (40μM) of the NMDA receptor EPSC recorded in the thalamic input to the LA at V_H=−40 mV (experimental conditions as in A). Inset shows the baseline NMDAR EPSC (1) and its block at the end of presynaptic stimulation in the presence of MK-801 (2). **(F)** Summary graphs of the experiments with MK-801 protocol in thalamic input (from 3 *wt* mice, n=7 neurons and 4 *TRPC5* null mice, n=8 neurons; ANOVA, *P*=0.9). **(G)** Representative traces of the asynchronous quantal EPSCs evoked in the thalamic input at V_H =−70 mV. **(H)** Cumulative amplitude histograms of asynchronous quantal events recorded in the thalamic input to the LA (from 3 *wt* mice, n=11 neurons and 4 *TRPC5* null mice, n=16 neurons). Error bars indicate SEM.

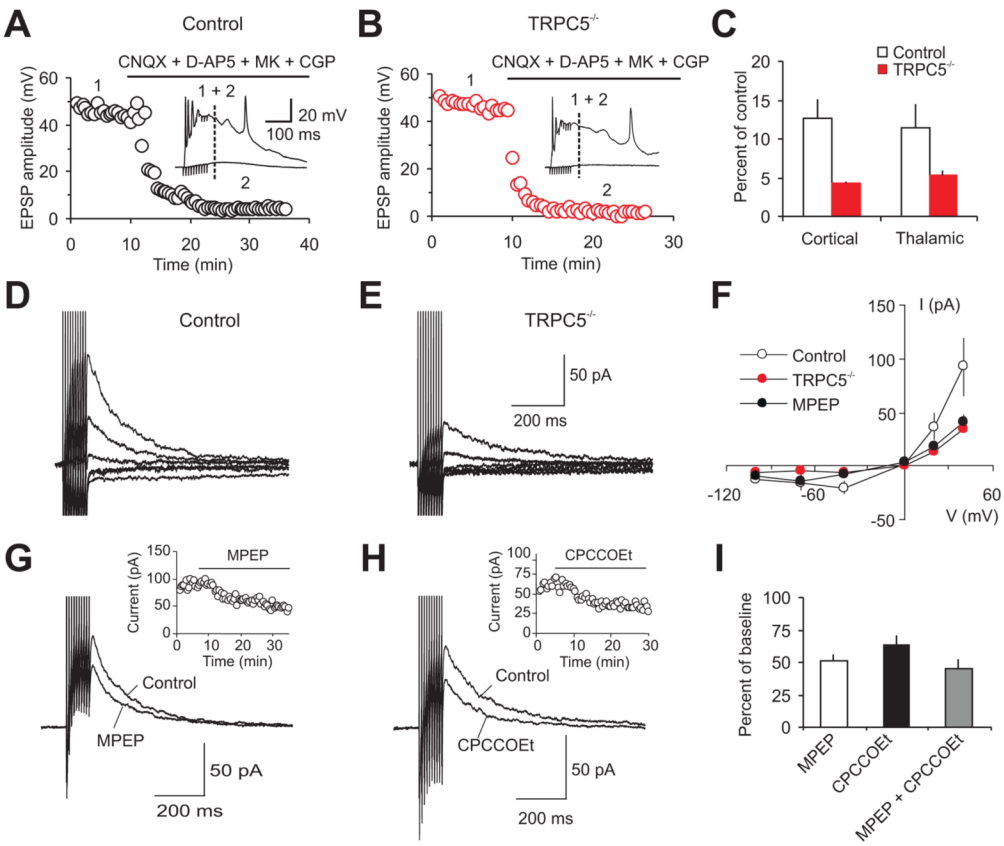

Figure 5. Synaptic responses mediated by mGluRs activation are diminished in *TRPC5*$^{-/-}$ mice

(A) Cortico-amygdala synaptic responses in brain slices from a control mouse evoked by trains of high frequency stimulation before and after addition of CNQX (AMPAR blocker; 20μM), NMDAR blockers D-APV (50μM) and MK-801 (10μm) and CGP 35348 ($GABA_BR$ blocker; 300μM). Stimulation trains consisted of 10 pulses at 100 Hz delivered once every 30s. Inset shows synaptic responses recorded in current-clamp mode before (1) and after (2) the addition of blockers to the external solution. The dashed line indicates the point where the EPSP amplitude was measured. **(B)** Experiment as in A), from a *TRPC5*$^{-/-}$ mouse. **(C)** Summary plot of the experiments shown in A) and B), performed in cortical and thalamic inputs to the LA. The amplitude of the residual component of the EPSP (measured at dashed line in A, B) in the presence of blockers was significantly smaller in both pathways in slices from *TRPC5*$^{-/-}$ mice (cortical input: from 7 *wt* mice, n=12 neurons, and 4 null mice, n=7 neurons. thalamic input: from 4 *wt* mice, n=8 neurons, and 5 null mice, n=11 neurons). **(D, E)** Short-train stimulation-induced cortico-amygdala EPSCs recorded at V_H ranging from −100 mV to +40 mV in slices from control (**D**) and *TRPC5*$^{-/-}$ **(E)** mice in the presence CNQX, D-APV, MK-801, CGP 35348 and picrotoxin (100μM). **(F)** Summary current-voltage (I/V) plots of the peak current in the cortical input (as in **D** and **E**), as well as from control mice in the presence of MPEP (10μM, filled black symbols). From 7 *wt* mice, n=11 neurons, and 3 null mice, n=7 neurons; from 4 *wt* mice in the presence of MPEP, n=4 neurons. **(G)** Short-train stimulation-induced cortico-amygdala EPSCs (V_H = +40 mV) are sensitive to the mGluR5 antagonist MPEP (10 μM). The inset shows the time course of MPEP block in slices from control mice. **(H)** A specific antagonist of mGluR1, CPCCOEt (40μM), also reduced the size of the slow EPSC. **(I)** Summary plot of the effects of MPEP (10μM, n = 4 cells from 3 *wt* mice, $P < 0.01$ versus baseline) and CPCCOEt (40μM, n=5 cells from 3 *wt* mice, $P<0.01$ versus baseline), and MPEP and CPCCOEt applied simultaneously (n=10 neurons from 7 *wt* mice); percent of EPSC

reduction induced by antagonists. *P*=0.34 for the effect of MPEP versus MPEP+CPCCOEt; *P*=0.16 for the effect of CPCCOEt versus MPEP. Error bars indicate SEM.

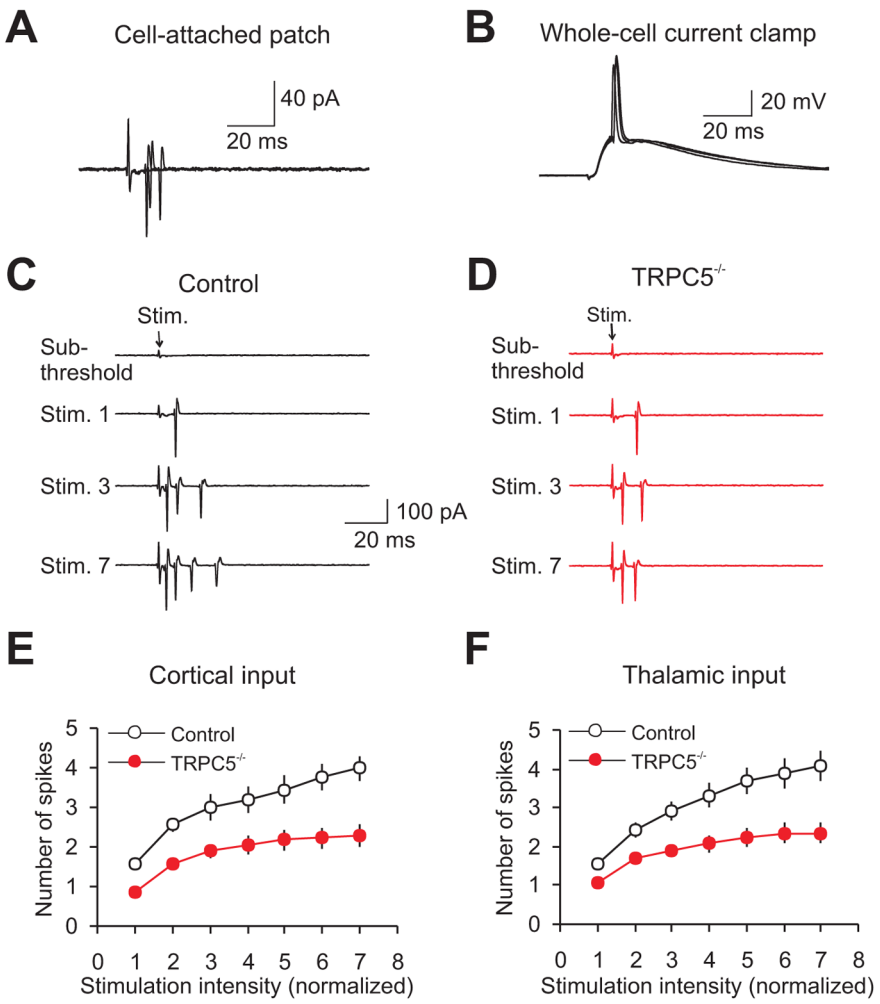

Figure 6. Firing output of neurons in the LA during synaptic activation is diminished in *TRPC5*$^{-/-}$ mice

(A) Superimposed postsynaptic responses (all-or-none extracellular spikes) evoked in a LA neuron by stimulation of the cortical input and recorded in a cell-attached patch configuration (as in Otmakhov et al., 1993). The recordings were performed in the presence of 50μM PTX and 2μM CGP55845. **(B)** Recordings under current clamp conditions at −70 mV from the same neuron as in A) after establishing a whole-cell recording configuration. **(C)** Examples of responses in the LA neuron (recorded in a cell-attached patch configuration) to stimulation pulses of increasing intensity, delivered to the cortical input in a slice from a control mouse. The intensity of stimulation was increased from the threshold stimulus required to elicit the spike, determined in each individual experiment, with an increment of 25μA. **(D)** Identical experiment as in C) but in a slice from a *TRPC5*$^{-/-}$ mouse. **(E, F)** The number of extracellular spikes evoked in LA neurons by presynaptic pulses of increasing intensity in cortical (**E**: from 4 *wt* mice, n=17 neurons and 4 *TRPC5* null mice, n=12 neurons; ANOVA, P=0.02) and thalamic (**F**: from 4 *wt* mice, n=16 neurons and 4 *TRPC5* null mice, n=15 neurons; ANOVA, P=0.02) pathways. First points represent responses evoked by the stimuli at the threshold +25 μA. Error bars indicate SEM.

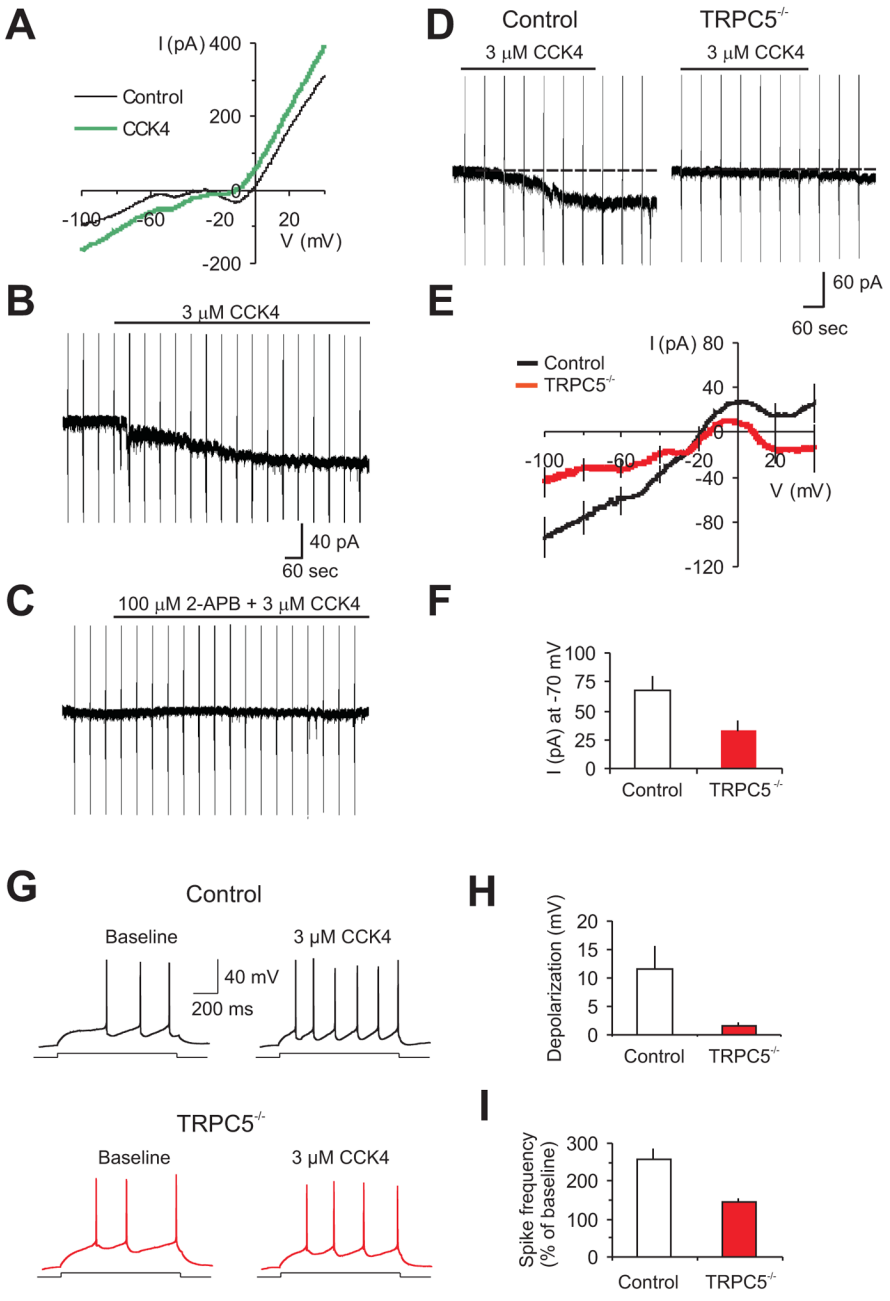

Figure 7. Membrane currents induced by activation of CCK2 receptors in LA neurons are diminished in *TRPC5*$^{-/-}$ mice

(A) Membrane currents induced in LA neurons (3.5s ramps from −100 to +40mV) under baseline conditions (black line), and after CCK4 agonism of CCK2 receptors (3μM, green line) in a control mouse. External solution also contained 0.5μM TTX, 200μM $CdCl_2$, and 50μM picrotoxin. ($[Ca2+]_i$ was buffered to 100nM; see Methods). **(B)** CCK4-induced current at V_H=−70mV, with voltage ramps applied every 60s; 66.9±12.9pA, n=9 cells from 4 *wt* mice. **(C)** 2-APB (100μM) abrogated CC4-induced membrane currents in LA neurons (2.5±1.4pA, n=4 cells from 3 mice, significantly different from CCK4 effects without the blocker, t-test, *P* =0.0079). **(D)** CCK4-induced currents in slices from *wt* (left) and *TRPC5*$^{-/-}$ (right) mice.

(E) Baseline-subtracted CCK4-mediated currents in LA neurons during ramps from −100 to +40mV (from 4 *wt* mice; n=9 neurons, and 6 null mice; n=8 neurons). **(F)** Averaged amplitudes of the CCK4-induced currents at −70 mV (from 4 *wt* mice, n=9 neurons, and 6 null mice, n=8 neurons, $P<0.05$). **(G)** Spikes evoked in LA neurons by current injection (150pA) recorded in current-clamp mode under baseline conditions and in the presence of 3μM CCK4. **(H)** CCK4-induced depolarization in LA neurons (from 2 *wt* mice, n=8 neurons, and 3 null mice, n=14 neurons). $P=0.005$ for depolarization in control mice versus depolarization in *TRPC5*$^{-/-}$ mice **(I)** Summary plot of the experiments as in (**G**), showing the percent increase in spike frequency in the presence of CCK4 relative to the baseline frequency (taken as 100%; n=8 neurons from 2 wt mice and n=14 neurons from 3 *TRPC5* null mice; t test, $P=0.004$). Error bars indicate SEM.